Screening ionization of excitons in photoexcited germanium

I. Balslev*
Max-Planck-Institut für Festkörperforschung, Heisenbergstrasse 1, D-7000 Stuttgart 80, Federal Republic of Germany
(Received 23 September 1983; revised manuscript received 30 April 1984)

The luminescence and absorption spectra associated with phonon-assisted transitions across the band gap are studied in laser-excited germanium in the temperature range 30—160 K. The resulting density of thermalized electron-hole pairs is determined from optical absorption below the absorption edge, and achieved values up to 1.2×10^{17} cm^{-3}. The experiments are compared with a model based on simple band extrema and a Yukawa-type interaction between electrons and holes. The Mott density defining the screening ionization limit of excitons is found from experiments to be $(3-4)\times10^{16}$ cm^{-3} in the temperature range 45—75 K. The measured and calculated absorption spectra do not agree in detail because of the neglect of band degeneracies in the model.

I. INTRODUCTION

The physics of photoexcited semiconductors with high density of electron and holes has been an important part of recent solid-state research. The observed phenomena are usually described by a modified independent particle approach. Here the concepts of electrons, holes, excitons, biexcitons, etc., are retained, but the energy gap and the excitonic ionization energies depend on the excitation density. Thus the coexistence of free excitons and the electron-hole liquid can be explained in detail on basis of statistical mechanics and zero-temperature calculations of the band renormalization in Fermi gasses of electrons and holes.[1-4]

The spatial separation between the excitonic phase and the electron-hole liquid prevents the study of a homogeneous, low-temperature metal-insulator transition discussed by Mott.[5] Above the critical temperature for the phase separation, the density-temperature diagram is divided into two regions separated by the Mott density n_M at which the Mott criterion is fulfilled.[5] For densities above n_M the system is a more or less degenerate gas of electrons and holes without exciton states. Below n_M there exist exciton states with finite-ionization energy, but the exciton states may be depopulated due to thermal ionization. In this work the boundary between these two systems will be called the screening-ionization limit rather than the Mott transition because the disappearance of finite radius exciton states does not necessarily lead to drastic changes of the electrical or optical properties.

Near and above the critical temperature for formation of the electron-hole liquid, there are several unanswered questions. First of all, it is uncertain whether the dilute side of the phase boundary has an extra pocket due to the Mott transition or a monotonous character with a continuous ionization of excitons.[6-10] Second, the excitation dependence for finite temperatures of the energy gap and the exciton-ionization energy is not fully established. Many-body theories[11,12] predict that a static Debye-Hückel model is a rather good high-temperature approximation, and that band renormalization and reduction of the exciton-ionization energy are essentially equal. However, an experimental verification of these features has been complicated by uncertainties in the determination of the band gap and the density of a Maxwellian gas of electrons and holes. Third, it is essential, but complicated to estimate how the free pairs influence the optical interband density,[13] i.e., the excitonic oscillator strengths and the Coulomb-enhanced pair continuum of the optical spectra. As demonstrated by Schmitt-Rink *et al.*[14] it is useful to derive the optical spectra directly from many-body calculations without explicit calculation of Coulomb enhancement, density of states, etc.

In order to gain more knowledge of the screening-ionization limit the following optical phenomena have been measured simultaneously in laser-excited germanium: (a) Optical absorption below the energy gap due to free electrons and holes. (b) Excitation-induced changes of the indirect absorption edge at and above the threshold for longitudinal acoustic (LA) phonon-assisted transitions. Similar studies at lower excitation densities are reported by Thomas *et al.*[15] and by the author.[16] (c) Photoluminescence similar to that reported by Schweizer *et al.*[10] (d) Induced changes in the direct absorption edge. Here the sample thicknesses used do not allow a complete study of the direct absorption edge in the manner of the one reported in Ref. 12.

In Sec. II the experimental methods and results are presented. In Sec. III the measured free-carrier absorption is related to previous studies on doped germanium,[17,18] thus obtaining the pair densities during photoexcitation. In Sec. IV the measured spectra near and above the indirect thresholds are discussed. It is demonstrated that the electron-hole system is pumped to well above the screening-ionization limit at the highest excitation level used. The Mott density derived from the spectra are compared with theoretical results. A Debye-Hückel screening model applied to a pair of simple band extrema is analyzed in the Appendix, but the calculated spectra are not in detailed agreement with the experiments. The reason for this is discussed in Sec. IV. In Sec. V the most important results of the work are summarized.

II. EXPERIMENTS

Specimens of high purity Ge with thickness 0.3—0.7 mm were mounted with silver paste on a 1-mm copper plate. The sample dimensions parallel with the plate was 5×0.7 mm^2, and the sample covered a 0.6-mm-diam pinhole on the copper plate. The arrangement was mounted in a helium-gas exchange cryostat, and two light sources were focused to fill the pinhole: a probing tungsten-halogen lamp and a pumping Nd:YAG laser (wavelength 1.05 μm, output power up to 6 W). The laser was mechanically chopped in such a way that the sample was illuminated 0.33 ms with a repetition rate of $f_1\cong300$ pps (duty cycle of 1:10). The tungsten lamp was ac powered with a frequency of $f_2\cong45$ Hz which gave a 1% modulation (at frequency $2f_2$) of the emitted light. The tungsten-lamp light transmitted by the sample was focused on the entrance slit of a monochromator followed by a PbS detector. By means of phase-sensitive detection with reference frequencies f_1 and $2f_2$ it was possible to produce a signal proportional to the relative modulation ($\Delta I/I$) of the tungsten-lamp light caused by the laser excitation. Owing to the slow response of the detector it was not possible to perform a time resolution of the signal. Some temporal information was obtained by recording the signal in phase and out of phase with the laser excitation.

Because the pump-pulse duration is much longer than the recombination times in Ge (<5 μs), there is an electronic steady state during the whole illumination period. Thus the transmission modulation caused by the electronic system has the same phase and temporal wave form as the laser illumination. On the other hand, the thermal effects (particularly thermal modulation of the band gap) having a much slower relaxation produce a signal with a component 90 degrees out of phase with the laser.

Out-of-phase signals are detectable at photon energies near and above the thresholds of the indirect absorption edge. They are similar to those of wavelength modulation[19] and assigned to a rigid, thermally induced shift of the absorption edge. These spectra are used for determination of the average phonon temperature via the spectral position of the threshold for LA-phonon-assisted transitions. An impression of the sample heating caused by the laser can be obtained from the following numbers: With a sample thickness of 0.35 mm and an average laser power of 0.5 W (peak power 5 W), the temperature increase in the sample was 20, 15, and 25 K for He gas temperatures of 10, 30, and 50 K, respectively. These results reflect the fact that the thermal conductivity in Ge has a maximum at 25 K.[20]

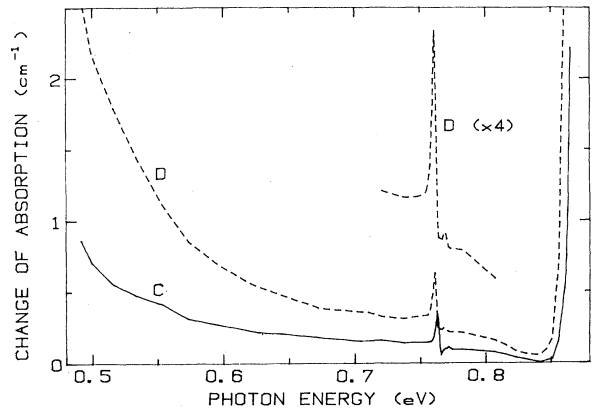

FIG. 2. Measured spectra of $\Delta\alpha$ with $T_{He}=50$ K and high excitation density [sample thickness 0.35 mm and external laser power equal to 2 W (curve *C*) and 5 W (curve *D*)].

Considering the small magnitude of the out-of-phase signal and the heat-diffusion times involved, it is concluded that the thermal contribution to the in-phase signal is small. Therefore, the isothermal change of the absorption coefficient $\Delta\alpha$ caused by the electron-hole pairs is derived from

$$\Delta\alpha d=-\ln(1-\Delta I/I)\,, \tag{1}$$

where d is the sample thickness and $\Delta I/I$ is the in-phase signal. In Eq. (1) the excitation dependence of the refractive index is neglected. At low temperatures the lumines-

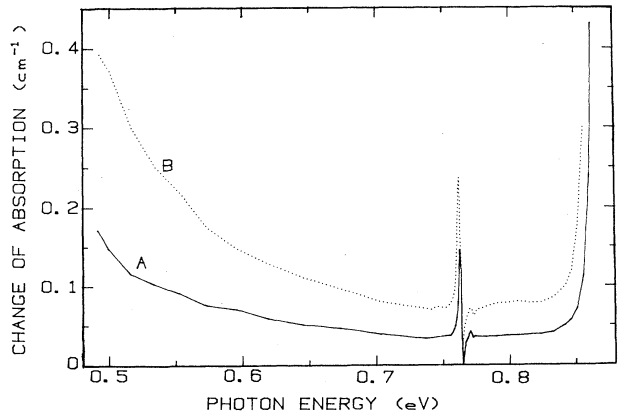

FIG. 1. Measured spectra of $\Delta\alpha$ with $T_{He}=50$ K and moderate excitation density [sample thickness 0.75 mm and external laser power equal to 2 W (curve *A*) and 5 W (curve *B*)].

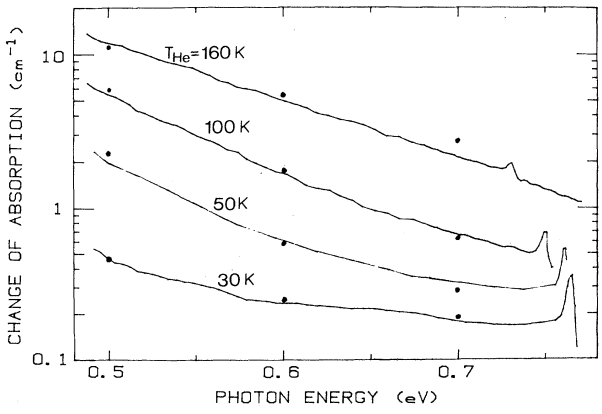

FIG. 3. Measured spectra of $\Delta\alpha$ (solid lines) with external laser power 5 W, sample thickness 0.35 mm, and different temperatures of the helium exchange gas. The dots are calculated results for pair densities given in Table I.

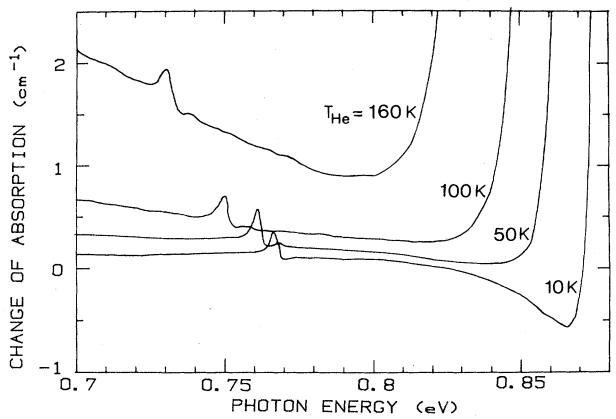

FIG. 4. Spectra as in Fig. 3 in a different spectral range.

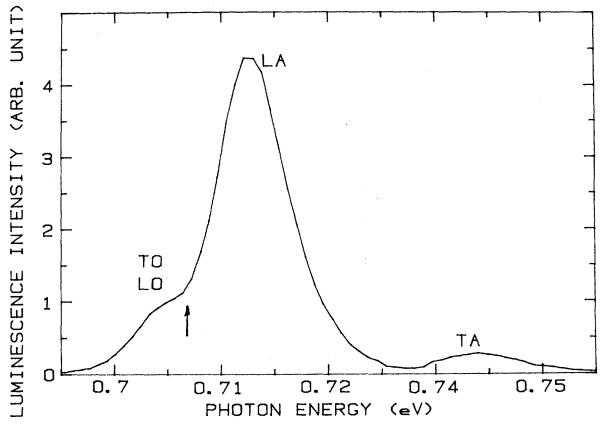

FIG. 5. Luminescence spectrum for $T_{He}=10$ K, $d=0.35$ mm, and an external laser power of 5 W. The sample temperature is 30 K.

cence recorded without a tungsten lamp is not negligible compared to the signal ΔI. In such cases the recorded transmission-modulation spectra are corrected accordingly.

Spectra of $\Delta\alpha$ in the photon-energy range 0.48—0.88 eV for various power levels, temperatures, and sample thicknesses are shown in Figs. 1—4. A single luminescence spectrum recorded at the highest excitation level is shown in Fig. 5.

III. FREE-CARRIER ABSORPTION

In this section the measured absorption below the indirect absorption edge is analyzed in terms of free-carrier absorption which is well explored in doped Ge. Experimental results on n- and p-type crystals agree in detail with theoretical studies of interband and intraband transitions.[17,18]

The absorption from free electrons in Ge is due to intraband transitions and given by a cross section which is well represented by the expression[17]

$$\sigma_e=\sigma_{e0}(\omega/\omega_0)^{-1.7}\,, \tag{2}$$

where ω and ω_0 are frequencies in the near-infrared region. With $\hbar\omega_0=0.25$ eV, σ_{e0} is about 1.2×10^{-17} cm^2 for electron densities below 10^{17} cm^{-3}.

In the region $\hbar\omega>0.3$ eV the absorption by free holes in Ge is dominated by direct interband transitions. The excitation of heavy holes to the spin-orbit split-off band is governed by the absorption cross section[18]

$$\sigma_h=\sigma_{h0}[\gamma(\hbar\omega-\Delta)/kT\,]^{3/2}\exp[-\gamma(\hbar\omega-\Delta)/kT\,]\,. \tag{3}$$

Here kT is the thermal energy, Δ is the spin-orbit splitting, and σ_{h0} and γ are parameters given by the valence-band effective masses. The absorption data for $T=77$ K by Newmann and Tyler[2] lead to the values of $\sigma_{h0}=2.7\times10^{-16}$ cm^2 and $\gamma=0.16$ for densities below 10^{17} cm^{-3}.

The measured absorption induced by the excitation is close to the expected result $\alpha=n(\sigma_e+\sigma_h)$ derived for temperatures equal to those found from the indirect absorption edge. n is the free-pair density, the values of which are fitted to the measurements. At low temperatures σ_h is small for $\hbar\omega>0.48$ eV and σ_{e0} is not well known. Therefore the present method for determination of n is unreliable for temperatures below 45 K.

The densities obtained for different temperatures and power levels are given in Table I. The calculated values of $n(\sigma_e+\sigma_n)$ are shown as dots in Fig. 3. As the excited volume is about 10^{-4} cm^3 and an external laser power of 5 W gives a production rate of 1.7×10^{19} pairs/s, it is seen that the density obtained ($\simeq10^7$ cm^{-3}) corresponds to a lifetime of the order 0.6 μs. This lifetime is found to be essentially independent of temperature and power level in the range investigated.

At the maximum density (1.2×10^{17} cm^{-3}) the pair chemical potential is estimated to be more than kT below the pair continuum if the sample temperature is greater than 30 K. Hence at all the temperatures studied the electron and hole gases are essentially Maxwellian.

TABLE I. Free-pair densities n and sample temperatures obtained from different excitation power levels and helium gas temperatures. The sample thickness is 0.35 mm.

Peak excitation power (W)	5	5	2	5	5	5
Average excitation power (W)	0.5	0.5	0.2	0.5	0.5	0.5
Helium-gas temperature (K)	10	30	50	50	100	160
Average sample temperature (K)	30	45	60	75	120	170
Free-pair density during excitation period (10^{17} cm^{-3})		1.1	0.6	1.2	1.2	1.1

IV. THE INDIRECT ABSORPTION EDGE

The spectra of $\Delta\alpha$ can be broken down into three contributions (see Figs. 1–4). First of all the free electrons and holes give rise to the absorption discussed in Sec. III. Second, the band renormalization of the direct gap produces a sharp rise in $\Delta\alpha$ at high photon energies ($\hbar\omega = 0.83$–0.87 eV depending on temperature). This contribution shall not be commented on further because the direct absorption edge in photoexcited germanium has been studied in detail previously.[12] Third, the change of the indirect absorption edge is noticeable near and above the indirect LA threshold at $\hbar\omega \approx 0.7$ eV.

This section is devoted to the last-mentioned contribution which is characterized by two important features. First, there is a sharp structure near the threshold for transitions assisted by emission of LA phonons. A weak satellite at slightly higher energy (see Figs. 1 and 2) is due to participation of optical phonons. Second, a structureless negative contribution above the LA threshold is clearly seen at high excitation levels and low temperatures. It is instructive to generate the resulting absorption coefficient by adding the zero excitation absorption reported in Ref. 22 to the presently measured spectrum of $\Delta\alpha$. The result of this is shown in Fig. 6. Here the free-carrier contribution is subtracted for clarity.

Let us now estimate the expected behavior of the indirect absorption with and without photoexcitation. For simple band extrema the indirect absorption edge at zero excitation is composed of phonon components given by[22]

$$\alpha \propto \sum_{n=1}^{\infty} \frac{E_{x0}}{n^3}(\hbar\omega - E_{g0} + E_{x0}/n^2 - E_p)^{1/2} + \tfrac{1}{3}(\hbar\omega - E_{g0} - E_p)^{3/2}, \quad (4)$$

where E_{x0} is the exciton binding energy, E_{g0} is the energy gap, and E_p is the phonon energy. Here and later in this work the term $(\hbar\omega - E)^q$ is taken to be 0 for $\hbar\omega < E$. The sum in Eq. (4) corresponds to creation of excitons, while the last term is caused by band-to-band transitions. As the individual exciton components are unresolved it is reasonable to lump them into a single component. Then,

$$\alpha \propto F E_{x0}(\hbar\omega - E_g + E_x - E_p)^{1/2} + \tfrac{1}{3}(\hbar\omega - E_g - E_p)^{3/2} \quad (5)$$

where the strength F, the exciton binding energy E_x, and the energy gap E_g are now considered as excitation-dependent quantities.

The density dependence of the energy gap E_g is studied by Zimmerman *et al.*[11] and by Schweizer *et al.*[12] using many-body treatments of the electron-hole system. Their results are well represented by

$$E_g - E_{g0} = -1.2\, E_{x0}(n/n_M)^{0.5}, \quad (6)$$

where n_M is the Mott density at which E_x becomes 0. The exciton binding energy E_x and the strength F of the excitonic component decreases with excitation and become 0 for $n > n_M$. These last-mentioned dependencies can be calculated within the effective-mass approximation by replacing the electron-hole Coulomb potential by a Yukawa potential

$$V(r) = -\frac{e^2}{\epsilon r}\exp(-k_s r) = -2E_{x0}(a_B/r)\exp(-k_s r), \quad (7)$$

where a_B is the exciton Bohr radius at zero excitation, k_s is a density-dependent screening constant, and r is the electron-hole separation. In a static Debye-Hückel model, k_s is given by[5]

$$k_s a_B = 1.2(n/n_M)^{1/2}, \quad (8)$$

and the Mott density n_M is given by

$$n_M = \frac{1.2^2 kT}{16E_{x0}} a_B^{-3}. \quad (9)$$

By inserting the potential of Eq. (7) in a usual Elliott treatment it is possible to calculate the dependencies of E_x and F on k_s. Such a treatment is discussed in the Appendix, and the results are shown in Fig. 7. The result for E_x compared with Eq. (6) has the consequence that the spectroscopic exciton energy $E_g - E_x$ is rather independent of excitation as also found in Refs. 11 and 12.

The change of absorption [Eq. (5)] with the pair density n can be expressed as

$$\frac{\partial\alpha}{\partial n} \propto \frac{\partial F}{\partial n}E_{x0}(\hbar\omega - E_g + E_x - E_p)^{1/2} - \frac{1}{2}\frac{\partial E_x}{\partial n}(\hbar\omega - E_g - E_p)^{1/2}, \quad (10)$$

where $\partial(E_g - E_x)/\partial n \approx 0$ is used. For $\hbar\omega - E_g \gg E_{x0}$, i.e., well above threshold Eq. (10) can be reduced to

$$\frac{\partial\alpha}{\partial n} \propto E_{x0}(\hbar\omega - E_g - E_p)^{1/2}[\partial(F - \tfrac{1}{2}E_x/E_{x0})/\partial n]. \quad (11)$$

The quantity $F - \frac{1}{2}E_x/E_{x0}$ is shown in Fig. 7 and is seen to be essentially constant between $k_s = 0$ and $k_s a_B = 0.6$. This explains the surprising fact that there is no overall

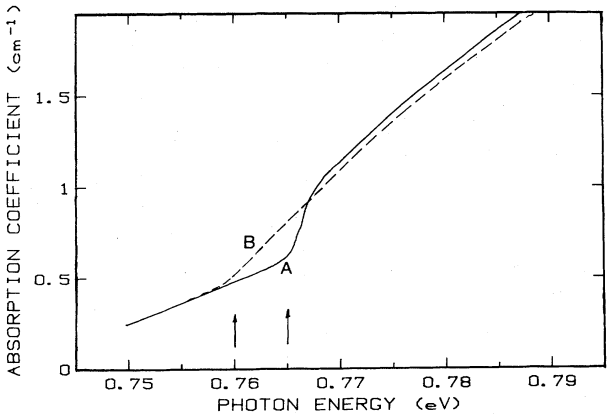

FIG. 6. Measured absorption coefficient near the LA threshold without excitation at $T = 45$ K (curve *A*) and with maximum excitation density at the same sample temperature (curve *B*). The free-carrier contribution is subtracted for clarity. The arrows show thresholds discussed in text.

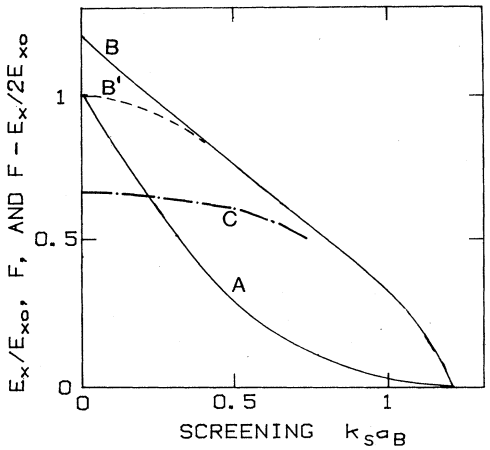

FIG. 7. Calculated screening dependence of the ground-state binding energy E_x (curve A) and the total excitonic oscillator strength F (curve B). The dashed curve (B') is the contribution to F from the $n=1$ exciton, and the curve C is the combination $F-E_x/2E_{x0}$ discussed in the text.

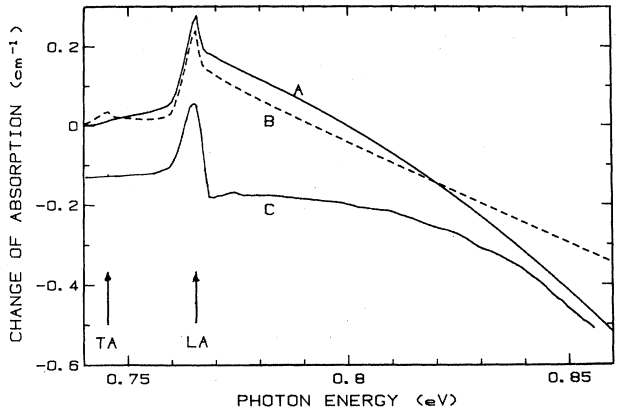

FIG. 8. Calculated and measured spectra of $\Delta\alpha$. Curve A is calculated with $k_s a_B=1.6$, $E_{g0}=0.743$ eV, $E_{g0}-E_g=9$ meV, and two phonon components: an allowed (LA) and a forbidden (TA) component with zero-excitation thresholds down. Curve C is measured with $T_{He}=10$ K and maximum excitation density. Curve B is calculated with the same input variables as curve A except that both phonon components are allowed. The strengths of the two phonon components in curves A and B are chosen to fit the zero-excitation absorption at low absorption levels ($\alpha<4$ cm^{-1}).

shift of the absorption edge at low and moderate excitation levels ($\Delta\alpha$ in Fig. 1 above the LA threshold has the same level as below, namely, that of the free-carrier absorption). In Ref. 6, F was considered as independent of n, and so the above cancellation between decreasing excitonic oscillator strength and the red shift of the pair continuum was not incorporated.

Turning to Fig. 6 it is seen that the highest excitation has caused the excitonic contribution of the LA component to vanish (no pronounced negative curvature on curve B above the LA threshold). This is an indication of a pumping level beyond the screening ionization. The threshold seen in the high-excitation spectrum at 0.760 eV is, therefore, the onset of band-to-band transitions. The zero-excitation threshold $E_{g0}-E_{x0}+E_p$ is 0.765 eV. Then, using $E_{0x}=4.0$ meV (Ref. 23) one obtains $E_{g0}-E_g=9$ meV at the excitation level shown in Fig. 6 ($n=1.1\times10^{17}$ cm^{-3}). From Eq. (6) one can interpolate and find the Mott density

$$n_M=3\times10^{16}\ \text{cm}^{-3} \tag{12}$$

at 45 K. This and the result for 75 K are displayed in Table II along with various theoretical estimates based on a zero-excitation Bohr radius of $a_B=11$ nm.[23] It is seen that the experimental values are slightly higher than obtained from the Debye-Hückel model and the calculations reported by Schweizer *et al.*,[12] while the calculations by Zimmermann *et al.*[11] give rather low Mott densities.

The above result that the band renormalization is 9 meV at the highest excitation level is confirmed by the luminescence spectrum in Fig. 5. Here the dominant LA component has a width which is roughly the same as that of the function $(\hbar\omega-E_g+E_p)^q\exp(-\hbar\omega/kT)$ with $q=\frac{3}{2}$. For infinite screening q should be 2. However, as shown in the Appendix, q is about $\frac{3}{2}$ in a wide range above n_M ($n_M<n<3n_M$). Therefore, the spectral point with maximum curvature at 0.707 eV is assigned to be the onset of band-to-band luminescence assisted by LA phonons. Then, using $E_{g0}-E_{x0}=0.739$ eV at 30 K and $E_p=0.0275$ eV,[22] the band renormalization is found to be 8.5 meV.

So far only the gross feature of the spectra near the indirect absorption edge have been discussed. A detailed quantitative analysis of the spectra should in principle provide more information than presented above. At very low excitation the line shape of $\Delta\alpha$ near the LA threshold is well explained by a density-dependent lifetime broadening.[15,16] However, a spectral analysis involving pair densities above n_M turns out to be more problematic. The spectra based on simple bands and Debye-Hückel screening deviate considerably from the measured spectra. This is demonstrated in Fig. 8 where the forbidden TA and the allowed LA components are incorporated in the calcula-

TABLE II. Mott densities calculated from various models compared with values obtained in the present experiments. The results from Ref. 12 have been scaled by using the values $E_{x0}=1.9$ meV and $a_B=27$ nm for direct excitons in Ge.

	$T=45$ K	$T=75$ K
Present experiments	3.0×10^{16} cm^{-3}	4.3×10^{16} cm^{-3}
Debye-Hückel model, Eq. (6)	2.1×10^{16} cm^{-3}	3.5×10^{16} cm^{-3}
Zimmermann *et al.* (Ref. 11)	0.9×10^{16} cm^{-3}	1.5×10^{16} cm^{-3}
Schweizer *et al.* (Ref. 12)	2.2×10^{16} cm^{-3}	2.8×10^{16} cm^{-3}

tions. Although the negative sign and the negative curvature of $\Delta\alpha$ above the LA threshold are reproduced by the theory, the fit is far from satisfactory. The most probable reason for this is that germanium does not have isotropic and nondegenerate band extrema as assumed in the model. Among the drastic consequences of the complex band extrema in germanium is the splitting and nonparabolicity of the $n=1$ exciton.[24] A detailed study of the overall shape of the absorption edge at zero excitation shows that the band-to-band absorption compared with the excitonic component is much weaker than given in Eq. (4). Until a tractable model is able to explain the zero-excitation absorption edge, it seems useless to refine the screening model for obtaining a better fit than shown in Fig. 8.

V. CONCLUSION

The present work can be summarized as follows.

(1) Pure germanium is optically pumped to contain more than 10^{17}-cm^{-3} electron-hole pairs in steady state. The density is determined by free-carrier absorption.

(2) The indirect absorption edge is explored in detail for different temperatures and pumping levels. With a suitable interpolation [Eq. (6)] between low and high excitation, the Mott density n_M is deduced from experiments (Table II). This is possible because the luminescence and the absorption spectra at high excitation have the characteristics of band-to-band transitions. The experimental results for n_M are slightly higher than found from the most recent many-body calculation[12] and from a Debye-Hückel model with constant spectroscopic exciton energy below n_M.

(3) The simple screening model used cannot be fitted accurately to the measured spectra of the indirect absorption edge probably because of the complex-band extrema in germanium.

ACKNOWLEDGMENTS

Fruitful discussions with M. Altarelli, M. Cardona, E. O. Goebel, H. Haug, and J. Wagner are gratefully acknowledged.

APPENDIX

The spectral shape of the indirect absorption edge and luminescence in a highly excited semiconductor can be calculated from a model involving simple band extrema and a Yukawa-type electron-hole potential.

For this purpose it is convenient to introduce a function $D(E_r,k_s)$ describing the optical-transition probability of a specific pair state. The pair state considered is characterized by the energy E_r associated with the relative electron-hole motion. Thus $E_r=-E_{x0}$ for unscreened $n=1$ excitons, and $E_r>0$ for the pair continuum. In case of direct transitions and an energy gap E_g^0, the function $D(\hbar\omega-E_g^0, k_s)$ is proportional to the spectral density of oscillator strength at frequency ω. In the absence of screening, Elliott[25] finds

$$D(E_r,0)=\sum_{n=1}^{\infty}\frac{1}{n^3}\delta\left[\frac{E_r}{E_{x0}}+\frac{1}{n^2}\right]+\frac{\Theta(E_r)/2}{1-\exp[-2\pi(E_{x0}/E_r)^{1/2}]}, \tag{A1}$$

where Θ is the unit step function. Note that $D(E_r,k_s)$ is normalized to be $\frac{1}{2}$ at the continuum limit ($E_r=0$) and zero screening ($k_s=0$). As in Ref. 13 the function D shall be called the optical-interband density although E_r rather than $\hbar\omega$ is used here as the independent variable. The present normalization is also different from that of Ref. 13. In case of full screening,

$$D(E_r,\infty)=\frac{1}{4\pi}(E_r/E_{x0})^{1/2}\Theta(E_r) \tag{A2}$$

corresponding to the joint density of states without Coulomb enhancement. The behavior of $D(E_r,k_s)$ for intermediate values of k_s has been explored by Dow.[26] He uses the Hulthén potential, which is slightly different from the Yukawa potential, and concentrates on the pair continuum.

In the present work $D(E_r,k_s)$ is calculated by numerical integration of Stahl's polariton equations with a lifetime broadening Γ incorporated. As will be shown in a later paper this method can be used above as well as below the continuum limit ($E_r=0$) and is very simple with respect to programming. The numerical calculations are reasonably fast for $\Gamma\geq 0.1E_{x0}$. Typical spectra of $D(E_r,k_s)$ for $\Gamma=0.1E_{x0}$ are shown in Fig. 9. These spectra are similar to those obtained from many-body calculations.[12] Note that the dependence of $D(E_r,k_s)$ on E_r is

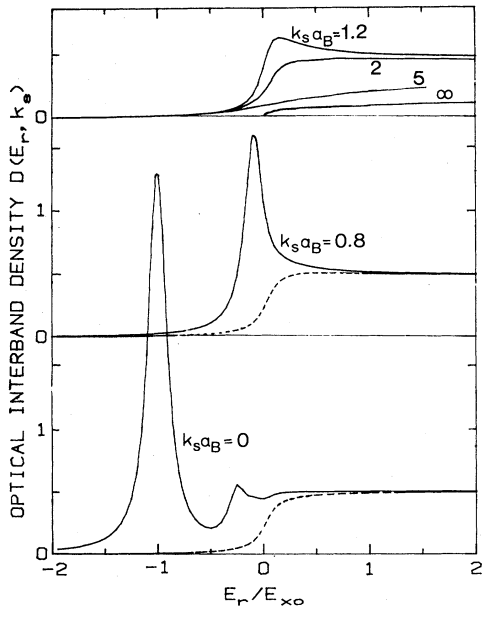

FIG. 9. Calculated spectra of the optical-interband density $D(E_r,k_s)$ for different screening constants k_s. The lifetime broadening Γ is $0.1E_{x0}$ [except for $k_s=\infty$ in which case Eq. (A2) is used]. The dashed curves shown for $k_sa_B<1.2$ are the contribution from the pair continuum.

essentially a broadened step function in the range of $1.2 < k_s a_B < 2$, and that the dependence in Eq. (8) normally used for an electron-hole plasma is only valid far above the Mott density. The total oscillator strength of the excitonic resonances, defined as

$$F(k_s) = \int_{-\infty}^{0} D(E_r, k_s) dE_r \, / E_{x0} \tag{A3}$$

is shown in Fig. 7. Also shown is the ground-state binding energy E_x versus $k_s a_B$ found by variational calculation.

The optical-interband density $D(E_r, k_s)$ is useful not only for absorption spectra of direct transitions, but also for luminescence and absorption spectra of phonon-assisted transitions. Thus, the pair creation assisted by emission of a phonon with energy E_p is governed by the absorption coefficient

$$\alpha \propto \int D(E_r, k_s) \delta(\hbar\omega - E_g - E_r - E_t - E_p) g(E_t) dE_t \tag{A4}$$

where $\hbar\omega$ is the photon energy, E_g is the renormalized indirect energy gap, and E_t and $g(E_t)$ are kinetic energy and density of states associated with the center-of-mass motion of the pair, respectively. Thus for a pair of simple band extrema

$$g(E_t) \propto E_t^{1/2} \Theta(E_t) \, . \tag{A5}$$

Equation (A4) is based on the assumption that the pair state created is essentially unoccupied before the transition (Maxwell-Boltzmann statistics).

In a wide spectral range the last term in Eq. (A1) can be approximated to a step function. Inserting this, the zero-excitation absorption can be calculated analytically [Eq. (4)].

Pair recombination assisted by phonon emission gives the spontaneous luminescence intensity given by

$$I_{\text{lum}} \propto \int D(E_r, k_s) \delta(\hbar\omega - E_g - E_r - E_t + E_p) \times g(E_t) f(E_r, E_t) dE_t \, , \tag{A6}$$

where $f(E_r, E_t)$ is the occupation probability of a pair state with relative and translational energies E_r and E_t, respectively. In case of Maxwell-Boltzmann statistics and $E_r \gg 0$,

$$f(E_r, E_t) \propto \exp[-(E_r + E_t)/kT] \, . \tag{A7}$$

It is convenient to discuss a few simple limits of Eqs. (A4) and (A6) in terms of the expressions

$$\alpha \propto (\hbar\omega - E)^q \, , \tag{A8}$$

$$I_{\text{lum}} \propto (\hbar\omega - E + 2E_p)^q \exp(-\hbar\omega/kT) \, . \tag{A9}$$

For the $n = 1$ excitonic component $q = \frac{1}{2}$ and $E = E_g - E_x + E_p$. For infinite screening $q = 2$ and $E = E_g + E_p$. In a wide density range just above n_M ($n_M < n < 3n_M$ corresponding to $1.2 < k_s a_B < 2$) the band-to-band contribution has $q = \frac{3}{2}$ and $E = E_g + E_p$.

All the above results concern allowed transitions. For forbidden transitions an extra E_t appears in Eqs. (A4) and (A6). This change gives values of the exponent q which are one higher than given above for allowed transitions.[22]

*Present address: Fysisk Institut, Odense Universitet, DK-5230 Odense M, Denmark.

[1]C. D. Jeffries, Science **189**, 955 (1975).
[2]T. M. Rice, in *Solid State Physics,* edited by H. Ehrenreich, F. Seitz, and D. Turnbull (Academic, New York, 1977), Vol. 32, p. 1.
[3]J. C. Hensel, T. G. Phillips, and G. A. Thomas, in *Solid State Physics,* edited by H. Ehrenreich, F. Seitz, and D. Turnbull (Academic, New York, 1977), Vol. 32, p. 88.
[4]P. Vashishta, P. Bhattacharyya, and K. S. Singwi, Phys. Rev. B **10**, 5108 (1974); P. Bhattacharyya, V. Massida, K. S. Singwi, and P. Vashishta, *ibid.* **10**, 5127 (1974).
[5]N. F. Mott, *Metal-Insulator Transitions* (Taylor and Francis, London, 1974), p. 124.
[6]T. M. Rice, in *Proceedings of the International Conference on Physics of Semiconductors, Stuttgart,* edited by M. H. Pilkuhn (Teubner, Stuttgart, 1974), p. 23.
[7]G. Mahler and J. L. Birman, Phys. Rev. B **16**, 1552 (1977).
[8]I. Balslev, Phys. Status Solidi B **101**, 749 (1980).
[9]L. J. Schowalter, F. M. Steranka, M. B. Salamon, and J. P. Wolfe, Solid State Commun. **44**, 795 (1982).
[10]H. Schweizer, A. Forchel, and W. Klingenstein, Phys. Status Solidi B **102**, 343 (1980).
[11]R. Zimmermann, K. Kilimann, W. D. Kraeft, D. Kremp, and G. Röpke, Phys. Status Solidi B **90**, 175 (1978).
[12]H. Schweizer, A. Forchel, A. Hangleiter, S. Schmitt-Rink, J. P. Löwenau, and H. Haug, Phys. Rev. Lett. **51**, 698 (1983).
[13]R. Zimmermann, M. Rösler, and V. M. Asnin, Phys. Status Solidi B **107**, 579 (1981).
[14]S. Schmitt-Rink, J. P. Löwenau, and H. Haug, Z. Phys. B **47**, 13 (1982).
[15]G. A. Thomas, A. Frova, J. C. Hensel, R. E. Miller, and P. Lee, Phys. Rev. B **13**, 1692 (1976).
[16]I. Balslev, Solid State Commun. **35**, 771 (1980).
[17]H. Y. Fan, W. Spitzer, and R. J. Collins, Phys. Rev. **101**, 566 (1956).
[18]A. H. Kahn, Phys. Rev. **97**, 1647 (1955).
[19]I. Balslev, Phys. Rev. **143**, 636 (1966).
[20]K. Seeger, *Semiconductor Physics* (Springer, Wien, 1973), p. 87.
[21]R. Newman and W. W. Tyler, Phys. Rev. **105**, 885 (1957).
[22]G. G. Macfarlane, T. P. McLean, J. E. Quarrington, and V. Roberts, Phys. Rev. **108**, 1377 (1957); T. P. McLean, in *Progress in Semiconductors,* edited by A. F. Gibson (Heywood, London, 1960), Vol. 5, p.53.
[23]M. Altarelli and N. O. Lipari, Phys. Rev. Lett. **36**, 619 (1976).
[24]A. Frova, G. A. Thomas, R. E. Miller, and E. O. Kane, Phys. Rev. Lett. **34**, 1572 (1975).
[25]R. J. Elliott. Phvs. Rev. **108**, 1384 (1957).
[26]J. D. Dow, in *Proceedings of the 12th International Conference on the Physics of Semiconductors, Stuttgart,* edited by M. H. Pilkuhn (Teubner, Stuttgart, 1974), p. 957.
[27]A. Stahl, Phys. Status Solidi B **106**, 575 (1981).
[28]A. Stahl and I. Balslev, Phys. Status Solidi B **113**, 583 (1982).